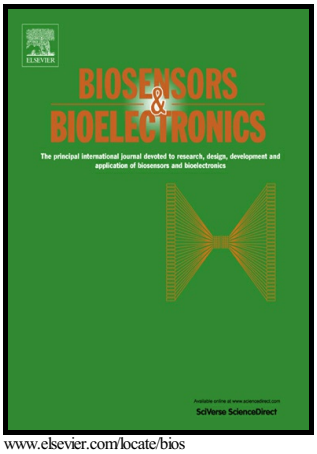

www.elsevier.com/locate/bios

Novel electrochemical biosensor based on PVP capped $CoFe_2O_4$@CdSe core-shell nanoparticles modified electrode for ultra-trace level determination of rifampicin by square wave adsorptive stripping voltammetry

Karim Asadpour-Zeynali, Fariba Mollarasouli

PII: S0956-5663(16)31110-1
DOI: http://dx.doi.org/10.1016/j.bios.2016.10.071
Reference: BIOS9293

To appear in: *Biosensors and Bioelectronic*

Received date: 9 September 2016
Revised date: 9 October 2016
Accepted date: 25 October 2016

Cite this article as: Karim Asadpour-Zeynali and Fariba Mollarasouli, Nove electrochemical biosensor based on PVP capped $CoFe_2O_4$@CdSe core-shel nanoparticles modified electrode for ultra-trace level determination of rifampici by square wave adsorptive stripping voltammetry, *Biosensors and Bioelectronic* http://dx.doi.org/10.1016/j.bios.2016.10.071

Novel electrochemical biosensor based on PVP capped $CoFe_2O_4$@CdSe core-shell nanoparticles modified electrode for ultra-trace level determination of rifampicin by square wave adsorptive stripping voltammetry

Karim Asadpour-Zeynali*, Fariba Mollarasouli
Department of Analytical Chemistry, Faculty of Chemistry, University of Tabriz, Tabriz 51666-16471, Iran

Abstract

This work introduces a new electrochemical sensor based on polyvinyl pyrrolidone capped $CoFe_2O_4$@CdSe core-shell modified electrode for a rapid detection and highly sensitive determination of rifampicin (RIF) by square wave adsorptive stripping voltammetry. The new PVP capped $CoFe_2O_4$@CdSe with core-shell nanostructure was synthesized by a facile synthesis method for the first time. PVP as a capping and etching agent for protection of the outer surface nanoparticles and formation of a mesoporous shell, respectively. Another important feature of this work is the choice of the ligand (1,10-phenanthroline) for precursor cadmium complex that works as a chelating agent in order to increases optical and electrical

* Corresponding author: K. Asadpour-Zeynali

Tel.: +98 413 3393113; Fax: +98 413 3340191.

E-mail address: asadpour@tabrizu.ac.ir; k.zeynali@gmail.com

properties and stability of prepared nanomaterial. The nanoparticles has been characterized by field emission scanning electron microscopy (FESEM), transmission electron microscope (TEM), energy dispersive X-ray spectroscopy (EDX), X-ray diffraction (XRD), UV–vis, photoluminescence (PL) spectroscopy, FT-IR, and cyclic voltammetry techniques. The PL spectroscopy study of $CoFe_2O_4$@CdSe has shown significant PL quenching by the formation of $CoFe_2O_4$ core inside CdSe, this shows that $CoFe_2O_4$ NPs are efficient electron acceptors with the CdSe. It is clearly observed that the biosensor can significantly enhance electrocatalytic activity towards the oxidation of RIF, under the optimal conditions. The novelty of this work arises from the new synthesis method for the core-shell of $CoFe_2O_4$@CdSe. Then, the novel electrochemical biosensor was fabricated for ultra-trace level determination of rifampicin with very low detection limit (4.55×10^{-17}M) and a wide linear range from 1.0×10^{-16} to 1.0×10^{-7}M. The fabricated biosensor showed high sensitivity and selectivity, good reproducibility and stability. Therefore, it was successfully applied for the determination of ultra-trace amounts RIF in biological and pharmaceutical samples with satisfactory recovery data.

Keywords: Rifampicin, Electrochemical biosensor, PVP capped $CoFe_2O_4$@CdSe magnetic nanoparticles, Glassy carbon electrode, Square wave adsorptive stripping voltammetry (SWASV)

1. Introduction

Rifampicin (RIF), 3-([(4-Methyl–1–piperazinyl) imino] methyl) rifamycin is an important antibiotic drug which is used in the treatment of several serious infectious such as tuberculosis, leprosy and HIV (Ramaswamy and Musser 1998). The mechanism of drug function is related to RIF binding to the RNA polymerase near its active center and prevents the initiation of RNA transcription by blocking formation of phosphodiester bond. Despite the some adverse effects such as nausea, hepatotoxicity, and allergic rashes, RIF has been widely used for the treatment many kinds of bacterial infection because it is more effective antibiotic than other antibiotics like isoniazid. Due to its toxicity in high concentration, it is

necessary to determine the drug levels in biological samples. Therefore, various analytical techniques have been used for determination of RIF in biological fluids and pharmaceutical formulations including high-performance liquid chromatography (HPLC) (Chellini et al. 2015; Goutal et al. 2016; Prasanthi et al. 2015), high performance thin layer chromatography (HPTLC) (Shewiyo et al. 2012; Védaste et al. 2014), liquid chromatography/tandem mass spectrometry (Vu et al. 2014), spectrophotometry (Mansuri et al. 2014), fluorescence (Liu et al. 2012), capillary zone electrophoresis (Faria et al. 2010), flow-injection chemiluminescence and voltammetry (Ajayi et al. 2014; Daneshgar et al. 2009; Gan et al. 2015; Gutiérrez-Fernández et al. 2004; Hammam et al. 2004; Kawde et al. 2014; Leandro et al. 2009; Lomillo et al. 2003; Lomillo et al. 2005; Rastgar and Shahrokhian 2014). Among these techniques, voltammetric methods based on electrochemical sensors have been extensively applied over the other because of advantages such as simplicity of sample preparation, low cost of instrumentation, miniaturization, high sensitivity, and selectivity. With increasing development of nanotechnology, nanoparticles have attracted special attention during recent decades due to their unique electrical, large surface-to volume ratio, optical and catalytic feature, and so their applications in electrochemical sensors have increased greatly.

Recently, quantum dots (0D) are one of the most attractive areas of nanotechnology because their size is very small about 2-10 nm in diameter due to quantum confinement. A specific type of fluorophores semiconductor that is composed of II-VI or III-V periodic elements and its radius is smaller than the bulk exciton Bohr radius is known as quantum dots (Azadbakht and Gholivand 2014). Quantum dots have broad applications including data storage (Kroutvar et al. 2003), drug delivery (Misra 2008; Probst et al. 2013), imaging (Misra 2008), light-emitting diode (Song et al. 2015), and most recently in fabrication of sensor and biosensor (Asadpour-Zeynali and Mollarasouli 2016). Although cadmium-based quantum dots may be toxic due to heavy metal, they can be easily bound to (bio) molecules by formation of complex. This problem can be resolved by using capping agents such as thioglycolic acid (TGA), penicillamine and polymeric layers, e.g., polyvinyl pyrrolidone (PVP) to reduce the toxicity of Cd-based QDs, increase the optical properties and stability. Capping agents also control the shape and size of nanoparticles by decreasing their growth rate to prevent aggregation. The use of an outer layer on the core of QDs and formation a core–shell structure is another approach in this case (Asadpour-Zeynali and Mollarasouli 2016).

The core–shell structure, consisted of a core (the central component) and a shell (the outer component), protects the core of QDs from adverse reactions such as oxidation and ion release that thereby improve the surface defects and increase of photostability. A core–shell structure is preferred with quantum dots as the shell and magnetic nanoparticles as the core in fabrication of (bio) sensor because of the ability of drug conjugation, superparamagnetic behavior, and biocompatibility.

Another important material in the nanotechnology is magnetic nanoparticles (MNPs) owing to their praise worthy magnetic properties. They have various applications including cell separation (Xu et al. 2011), drug delivery (Wu et al. 2011), enzyme immobilization (Ren et al. 2011), and protein purification, due to their ability to be detected and manipulated by an external magnetic field and redispersed rapidly in the absence of it. Among these, $CoFe_2O_4$ NPs as a type of excellent spinel ferrite can be good candidates for biomedical applications including cell labelling, magnetic resonance imaging (MRI) (Wu et al. 2011), tumor hyperthermia (Kashevsky et al. 2008), immunosensors (Tang et al. 2007) and magnetic fluids recording due to resistance to oxidation, chemical stability, mechanical hardness, high effective anisotropy, extremely low solubility, and moderate saturation magnetization (Varma et al. 2008). Sevral methods have been developed to synthesize this material such as sol–gel (Xu et al. 2008), citrate precursor method (Rashad et al. 2008), precipitation, micro-emulsion (Kahn and Zhang 2001), polymer complex (Montemayor et al. 2005) and hydrothermal process (Zhang et al. 2011).

In the present article, we offer initially a useful summary of the successful method for the synthesis of high quality PVP capped $CoFe_2O_4$@CdSe, which a layer of CdSe quantum dots was grown in situ around the $CoFe_2O_4$ magnetic nanoparticles to form a core–shell structure. We used poly (vinyl pyrrolidone) (PVP) as a capping agent and 1, 10-phenanthroline as a chelating ligand to form precursor cadmium complex. The use of PVP not only causes to protect the outer surface of $CoFe_2O_4$@CdSe but also makes the formation of a mesoporous shell because PVP can react with sodium hydroxide to form porous gels. In addition, both PVP and 1, 10-phenanthroline (phen) play a significant role in controlling the particle size and shape. The polymer coating of quantum dots has been considered a powerful instrument for detecting and sensing applications. Our research work reports the development of core-shell nanomaterials based on the use of biocompatible polymers (PVP) and combining organic ligands (1, 10-phenanthroline) for a novel biosensor applications. For this purpose, the synthesized PVP capped $CoFe_2O_4$@CdSe was cast on the surface of glassy

carbon electrode to fabricate the novel electrochemical biosensor (PVP capped $CoFe_2O_4$@CdSe/GCE) for the determination of RIF. The electrochemical oxidation of RIF at the PVP capped $CoFe_2O_4$@CdSe shows higher signals than those at the bare GCE and the $CoFe_2O_4$/GCE, revealing the excellent electrocatalytic activity of this film due to large surface area, abundant active sites and adsorptive capacity of PVP capped $CoFe_2O_4$@CdSe. Additionally, the developed sensor was applied to determine ultra-trace amounts of RIF in pharmaceutical and human blood serum samples using square wave adsorptive stripping voltammetry (SWASV).

2. Experimental

2.1 Apparatus and software

Voltammetric experiments were performed on a Metrohm 757 VA processor computerized electrochemistry instrument equipped with a three-electrode cell. Three–electrode system was employed for the electrochemical experiment, containing a saturated calomel electrode (SCE) as a reference electrode, a PVP-capped $CoFe_2O_4$@CdSe modified glassy carbon electrode as a working electrode (2.0 mm diameter for unmodified glassy carbon electrode), and a platinum counter electrode. A digital pH/mV/ion meter (Metrohm 827 pH Meter, Utrecht, The Netherlands) with a combined glass electrode was used for pH adjustment. Morphological images of PVP-capped $CoFe_2O_4$@CdSe-phen were characterized using a LEO 906 transmission election microscope (TEM, Zeiss, Germany) with an acceleration voltage of 100 kV. The field emission scanning electron microscopy (FESEM) and energy dispersive X-ray spectroscopy (EDX) were studied by a Tescan Mira3 FESEM with gold coating equipped with an EDX system. The X-ray powder diffraction (XRD) was carried out by a Rigaku D/max-2200X-Ray Diffractometer (Bruker AXS) using a Cu Kα source (λ=0.154056nm). Fourier transform infrared (FTIR) analysis was done by a Bruker FTIR spectrometer at room temperature (26 °C ± 1° C). The photoluminescence (PL) spectra were carried out on a Perkin-Elmer LS45 fluorescence spectrometer. UV–visible studies were recorded with an Avantes diode array spectrophotometer.

2.2 Synthesis of PVP-capped $CoFe_2O_4$@CdSe-phen

A solution of $CdCl_2$. H_2O (4 mmol, 0.0805 g dissolved in dry ethanol) was added drop by drop to the solution of 1,10-phenanthroline (phen, 4mmol 0.08g dissolved in dry ethanol) as a complexing agent in a three-neck round-bottom flask under stirring and nitrogen

atmosphere conditions. After this solution was stirred for 30 min at room temperature in nitrogen atmosphere, the white complex ($Cd(phen)Cl_2$) was produced. Then, 10 mL of PVP (3%, dissolved in dry ethanol) was added drop by drop to the above complex solution. After several minutes, 10 mL of 6.0 $molL^{-1}$ NaOH solution was injected into this mixture and kept for 1 h under stirring. At that moment, 10 mL of Fe^{3+}/Co^{2+} mixture (prepared from 0.108 g $FeCl_3 \cdot 6H_2O$ and 0.0485 g $CoCl_2 . 6H_2O$ in 10 ml deionized water) was added dropwise and pH adjusted in 12.0. Finally, 20 mL of 10×10^{-3} $molL^{-1}$ NaHSe (prepared from the reaction of Se powder with $NaBH_4$ in deionized water and nitrogen atmosphere) was quickly added to this mixture to obtain CdSe guantum dots. Subsequently, the obtained solution was refluxed at 95°C for 8h to form PVP-capped $CoFe_2O_4$@CdSe-phen. The final molar ratios of Cd^{2+}/Se^{2-}/Fe/Co/phen for the preparation of optimum MNPs@QDs were 2:1:2:1:2. After the end of the synthesis time, the obtained product was cooled. Subsequently, the dark magnetic precipitate was washed three times with water-ethanol mixture (1:1 v/v) to remove the unreacted reactants and collected by centrifugation at 4000 rpm for 10 min. Finally, it was dried in an oven at 40°C and stored in a dark place before use.

2.3 Preparation of modified GCE

Before modification, the surface of the electrode was first polished with 0.3 μm alumina slurry on a polishing cloth to mirror-like, and then rinsed with deionized water. After polishing, the GCE was ultrasonicated in ethanol and deionized water (1:1, v: v) for 10 min, to remove the remaining of alumina particles from the electrode surface. A certain amount of PVP-capped $CoFe_2O_4$@CdSe-phen (5 mg/ml) was dispersed in deionized water by ultrasonication for 1 h. Modified GCE was prepared by drop coating 10 μL of the above suspension on the surface of the cleaned GCE and allowed to evaporate water overnight at room temperature, to obtain a uniform film on the GCE surface. After modification, the obtained sensor is thoroughly rinsed with water and is ready for use. The sensor was immersed in a deoxygenated electrolyte solution.

3 Results and Discussion

3.1. Characterizations of the structure and morphology

The morphology of the synthesized PVP capped $CoFe_2O_4$@CdSe NPs was studied by FESEM, TEM, and EDX (Fig. 1A–K). Fig. 1A-D demonstrate the detailed structures of needle-like $CoFe_2O_4$ magnetic NPs without PVP at different magnification level. The size

distribution of the $CoFe_2O_4$ nanoparticles is almost homogeneous and their diameter is about 18–20 nm. Fig. 1E, F and G show the FESEM images of CdSe and $CoFe_2O_4$@CdSe nanocrystals, respectively. It is observed that CdSe QDs are embedded in PVP matrix and have uniform spherical colloidal crystallites with an average size of 13± 2. The nanocrystals are clearly well identified and no aggregation or agglomeration is observed, indicating effective capping of PVP on the surface of PVP capped CdSe NPs. Also from compare Fig. 1A and G, it is clear that PVP as a capping agent plays an important role in controlling the shape and size of the nanoparticles by decreasing the particle growth rate.

To further confirmation of the core@shell nanostructure, the morphology of PVP-$CoFe_2O_4$@CdSe core@shell nanoparticles dispersed in water was also investigated by TEM (shown in Fig. 1H-J). The existence of the dark areas (inner layer, core) and bright areas (outer layer, shell) in TEM images indicates the core@shell nanostructure of $CoFe_2O_4$@CdSe. A slightly agglomeration phenomenon observed in the TEM images may be due to magnetic properties of the synthesized particles and swelling of PVP in aqueous solution. In addition, the TEM images reveal that the as prepared nanoparticles are almost uniform and the mean size of the nanoparticles is approximately 12 nm.

Furthermore, the elemental composition of the PVP capped $CoFe_2O_4$@CdSe nanostructures was investigated by using an energy dispersive X-ray (EDX) attached to the scanning electron microscope presented in Fig. 1K. In EDX spectrum of PVP capped $CoFe_2O_4$@CdSe, only Cd, Se, Co, Fe, O and N elements were detected indicating that the PVP capped $CoFe_2O_4$@CdSe were successfully synthesized. Moreover, the relative areas of the peaks of Se and Cd are obtained to be about 0.28:0.49, so the atomic ratio of Se:Cd is about 1:2. Other characterizations of the PVP-capped $CoFe_2O_4$@CdSe such as XRD, IR and optical analysis are given in the Electronic Supplementary Material File.

3.2. Electrochemical behavior of rifampicin at the PVP-capped $CoFe_2O_4$@CdSe

To investigation the electrochemical behaviour of RIF on the $CoFe_2O_4$@CdSe/GCE, the voltammetric response was compared with the bare and modified glassy carbon electrode with $CoFe_2O_4$ magnetic nanoparticles (Fig. 2A). The cyclic voltammetric behavior of 10.0 μM RIF in 0.1M PBS pH 2.0 in the positive scan direction shows a quasi-reversible pair corresponding to redox peaks of hydroquinone group and an irreversible peak at higher potential related to oxidation of phenolic hydroxy group of RIF at both $CoFe_2O_4$/GC and $CoFe_2O_4$@CdSe/GC electrodes (curves b and c). At the bare GC electrode (curve a), a very

poor oxidation peak was observed at +416 mV, while after the modification of GCE surface with $CoFe_2O_4$, the anodic peak potential negatively shifted to +340 mV accompanied by an increase in peak current. In addition, the redox peak of RIF at the $CoFe_2O_4$@CdSe/GCE becomes reversible and appears at +219 mV and +200 mV for oxidation and reduction peaks, respectively, with a remarkable increase in peak current compared to $CoFe_2O_4$/GCE (about 60%). The enhanced signals and low peak separation potential (+19 mV) indicate that the $CoFe_2O_4$@CdSe/GCE improves electrochemical reactivity towards the redox reaction of RIF as compared with two other electrodes, probably due to facilitated the electron transfer rate and large effective surface area.

On the other hand, the $CoFe_2O_4$@CdSe/GCE has high electro-catalytic ability for the redox reaction of RIF owing to the high electron transfer rate (ks) obtained for RIF due to the decreased charge transfer resistance, and specific mesoporous structure that provides more active sites for further accumulation of RIF (see supplementary material file). In addition, interaction between RIF and PVP via formation of hydrogen bonds between carbonyl group of PVP and hydroxyl and amino groups of RIF can lead to strong adsorption of analyte on the electrode surface. Therefore, the sensitivity of RIF determination increases (Gan et al. 2015; Rastgar and Shahrokhian 2014; Roushani and Abdi 2014).

Fig. 2B describes the SWASV responses of 1.0×10^{-12} mol L^{-1} RIF on the above-mentioned electrodes at the same conditions. As can be seen, the response of $CoFe_2O_4$@CdSe/GCE was sharp, well defined and much higher than that of $CoFe_2O_4$/GCE and bare GCE.

3.3. Effect of type and pH of the supporting electrolyte

Rifampicin is an amphoteric drug with two pK_a values including pK_{a1} =1.7 and pK_{a2} = 7.9 related to the 4 hydroxyl group and the 3-piperazine nitrogen, respectively. The influence of the pH on the response of the CdSe@$CoFe_2O_4$ NPs/GCE towards 10μM RIF was investigated by cyclic voltammetry over the range from pH 1.0 to 7.0 in 0.04 M B–R buffer solutions. As can be seen in Fig. 3, the peak current and potential were changed with increasing pH value, indicating that the electrooxidation of RIF was pH-dependent. The maximum peak current was observed at pH 2.0 and then decreased when the pH values higher than 2.0. This behavior may be explained by this fact that the rifampicin molecule was protonated at pH < pKa (approximately at pH < 2.0), whereas at pH higher than 3 it is deprotonated and negatively charged. On the other hand, the electrode surface has negative

charge because of the carbonyl group which can interact with RIF at pH=2.0. Therefore, pH=2.0 was selected as an optimum pH for RIF in all voltammetric determinations.

The relationship between the formal potential ($E^{0'}$) and pH was also investigated. A linear shift of $E^{0'}$ towards less positive potential with the increasing pH from 1.0 to 7.0 was observed and it was shown as the following equation: $E^{0'}$ (V) = 0.33 - 0.0514 pH (R^2 = 0.9963). According to the Nernst equation (Eq. 1),

$$E^{0'} = E^{0} - \frac{2.303\ RTmpH}{nF} \quad (1)$$

m and n are the transference numbers of proton and electron, respectively; the $E^{0'}$-pH slope of RIF was obtained 51.4 $mVpH^{-1}$ which is close to the theoretical value of 59.2 $mVpH^{-1}$. This slope indicates that the numbers of electron and proton transferred were equal.in the redox reaction of RIF (reaction I).

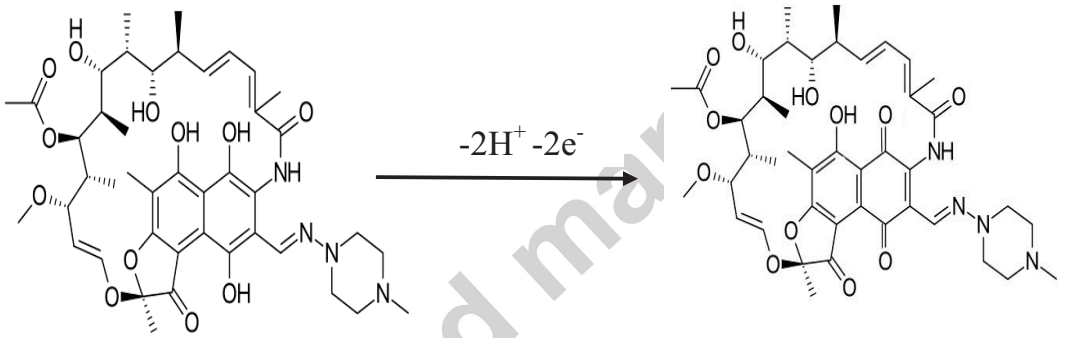

(I)

Rifampicin (RIF) Rifampicin quinone (RIF-Q)

3.4. Optimization of analytical conditions

In order to obtain the best stripping signal, the effective parameters for optimization including the solution pH, supporting electrolyte, the accumulation potential and time were studied before the voltammetric determination of RIF

3.4.1 The Effect of Accumulation pH

The effect of pH (1.0–8.0) on the adsorptive stripping current of 1.0×10^{-8} M RIF at $CoFe_2O_4$@CdSe/GCE was investigated. It was found that the maximum response of adsorptive stripping peak current appeared at pH 3.0. The effect of supporting electrolyte was also studied. Therefore, PBS (pH 3.0) was used as the supporting electrolyte in the preconcentration step (Fig. 4A).

3.4.2 The Effect of Accumulation Potential

The influence of the accumulation potentials (E_{acc}) on stripping peak currents of RIF was investigated using SWV in the range of 0 to -0.9 V for 1.0×10^{-8} M RIF in 0.1 M PBS at pH 3.0. As can be seen from Fig. 4B, for an accumulation time of 600s, the anodic peak current increased sharply with increase accumulation potentials from 0 to -0.7 V vs. SCE which reached a maximum at -0.7 V. When the accumulation potential becomes more negative than -0.7 V, the peak currents decreased due to evolution of hydrogen or the reduction of other compounds at more negative potential. They may interfere in the detection of RIF by the hydrogen bubble, which lead to decrease in peak current. Therefore, the potential -0.7 V was selected as an optimum accumulation potential for RIF.

3.4.3 Effect of the Accumulation Time

The effect of the accumulation time at −0.7V on the stripping peak current was also studied by recording square wave voltammograms at different accumulation times for 1.0×10^{-8} mol L^{-1} of RIF using a scan rate of 50mVs^{-1}. Fig. 4C shows that the oxidation peak current increased gradually with increasing the accumulation time from 30 to 600 s and then becomes constant at period longer than 600 s, presumably due to the saturated adsorption of RIF at the electrode surface. Considering both sensitivity and work efficiency, the accumulation time of 10 min is selected for the determination of RIF in the following experiments.

3.4.4 Effect of square wave parameters

Square wave voltammetry was used as powerful and simple electrochemical technique for low concentration determination of RIF. The peak current obtained in SWV is dependent on various instrumental parameters, such as the SW amplitude (ΔEa), scan increment (DEs) and SW frequency (f). By increasing the frequency from 10 to 100 Hz, the peak current increases, and shifts towards the positive potentials with a distortion in peak shape and an increase in the background current. The sensor exhibits the higher current response with increasing the pulse amplitude from 25 to 100mV but the background signal also increases. The best conditions for determination of RIF were then selected at 25 Hz frequency, 5 mV s^{-1} step potential with 50 mV pulse amplitude.

3.5. Calibration plot and limit of detection

Determination of RIF was performed using square wave anodic stripping voltammetry (SWASV) technique at different concentrations ranging from 0.1 fM to 0.1 μM in PBS (pH=2.0). Fig. 5 shows the square wave stripping voltammograms of the different concentrations at the CdSe@$CoFe_2O_4$/GCE. It is found that the peak current increased with the RIF concentration in the range of 10^{-16} to 10^{-7} mol/L and the calibration equation was $logI_{pa}$ (mA) = 0.0028 + 0.2185 logC (mmol/L) with a correlation coefficient of 0.9975. The limits of detection (LOD) and quantification (LOQ) were estimated to be 4.55×10^{-17} and 1.52×10^{-16}, respectively using the relation ks/m, where s is the standard deviation of the peak currents for the blank (n = 11), m is the slope of the calibration curve, k = 3 for LOD and 10 for LOQ (Miller and Miller 1993). Furthermore, a relative standard deviation of 1.72% (n=6) was obtained at the 1.0×10^{-10} mol L^{-1} rifampicin concentration level. The comparison of our sensor with other reported sensors in determining RIF is summarized in Table S1,

3.6. The reproducibility and stability of PVP-capped $CoFe_2O_4$@CdSe

The reproducibility of the developed sensor was evaluated by fabrication six electrodes in a completely same procedure described in the Electronic Supplementary Material File. The relative standard deviation (RSD) for the peak current of between electrodes is 2.62% of RIF that demonstrates an acceptable reproducibility for the fabrication procedure. The repeatability was examined by performing 6 times determination of same standard solutions (1.0×10^{-10} mol L^{-1} of RIF). The RSD of the peak signals was obtained to be 1.72%, indicating an excellent repeatability for PVP-capped $CoFe_2O_4$@CdSe/GCE. When the sensor was stored in air for two weeks, the peak current of it remained up to 97.2% of its initial response. Therefore, the developed sensor is suitable for the routine analysis of RIF in biological fluids and pharmaceutical dosage.

3.7. Interference studies

To evaluate the selectivity of the proposed sensor, the effect of the major potentially interferents frequently found with rifampicin in pharmaceutical formulations and in the biological fluids such as isonizide, pyrazinamide, uric acid, ascorbic acid, L-Threonine, and glucose on the SWV response of RIF at 1×10^{-8} mol/l level was performed under the optimum conditions. The results indicate that 2000-fold of glucose and L-Threonine, 1000-

fold of isoniazid and pyrazinamide, 500-fold of uric acid and ascorbic acid have no change in the stripping signal of RIF. This implies that the developed sensor exhibits excellent selectivity for the determination of RIF may be due to the specific mesoporous structure of PVP-capped $CoFe_2O_4$@CdSe and abundant active sites for adsorption of RIF by forming hydrogen bonds between carbonyl group of PVP and hydroxyl and amino groups of RIF, which it can match on the surface sensor.

3.8 . Sample analysis

The PVP-capped $CoFe_2O_4$@CdSe sensor was used to determine rifampicin in the tablet and human serum samples using the proposed SWASV and the standard addition method. As shown in Table 1, the recovery data of the sensor are in the range of 98.68–99.73% (RSD < 1.94%) and 97.36–101.45% (RSD < 3.32%) for analysis of tablet and serum samples, respectively, indicating the good precision and repeatability of the SW voltammetric determination of RIF using the PVP-capped $CoFe_2O_4$@CdSe/GCE. The obtained results for the average value of RIF are very close to the expected value, indicating the matrix does not lead any interfering effect on the voltammetric response of PVP-capped $CoFe_2O_4$@CdSe/GCE toward RIF. Therefore, the proposed sensor can be applicable in the determination of ultra-trace amounts RIF in real samples with different matrices.

4 Conclusion

In this work, a facile, novel, and versatile approach for synthesis of PVP-capped $CoFe_2O_4$@CdSe was introduced to fabricate an electrochemical sensor. $CoFe_2O_4$@CdSe/PVP was successfully applied to modify the surface of glassy carbon electrode for sensing of RIF via its electrochemical oxidation. Owing to the specific mesoporous structure of shell using PVP, the sensor achieves highly efficient accumulation ability and large effective surface area. The results show that after electrode modification, the oxidation signal of RIF was remarkably improved. Moreover, the prepared sensor has long time stability, simple and easy preparation of the sensor, high sensitivity, reproducibility of the voltammetric signals, and relatively low cost compared with other previous works. Therefore, such a sensor was proposed for the determination of ultra-trace amounts RIF, which was successfully confirmed with the determination of pharmaceutical and biological samples. In addition, the use of a sensitive technique (SWASV) can be an alternative to other techniques such as spectroscopy and HPLC, which determination of the analyte in complex matrices with these techniques,

require too expensive and complex equipment and or spending a long time. The wide linear range, biocompatibility, very low detection limit, good selectivity, and high electrochemical performance of the PVP-capped $CoFe_2O_4$@CdSe make it a promising candidate as a novel platform for fabrication of electrochemical biosensors and further sensor applications.

Acknowledgement

The authors wish to thank the financial support from the University of Tabriz, Tabriz, Iran. Authors would like to thank Dr. Masih Darbandi from University of Tabriz for his valuable help.

References:

Ajayi, R.F., Sidwaba, U., Feleni, U., Douman, S.F., Tovide, O., Botha, S., Baker, P., Fuku, X.G., Hamid, S., Waryo, T.T., 2014. Chemically amplified cytochrome P450-2E1 drug metabolism nanobiosensor for rifampicin anti-tuberculosis drug. Electrochim. Acta 128, 149-155.

Asadpour-Zeynali, K., Mollarasouli, F., 2016. A novel and facile synthesis of TGA-capped CdSe@Ag2Se core-shell quantum dots as a new substrate for high sensitive and selective methyldopa sensor. Sens. Actuators B Chem. 237, 387-399.

Azadbakht, A., Gholivand, M.B., 2014. Covalent attachment of Ni-2, 3-pyrazine dicarboxylic acid onto gold nanoparticle gold electrode modified with penicillamine-CdS quantum dots for electrocatalytic oxidation and determination of urea. Electrochim. Acta 125, 9-21.

Chellini, P.R., Lages, E.B., Franco, P.H., Nogueira, F.H., César, I.C., Pianetti, G.A., 2015. Development and Validation of an HPLC Method for Simultaneous Determination of Rifampicin, Isoniazid, Pyrazinamide, and Ethambutol Hydrochloride in Pharmaceutical Formulations. J. AOAC Int. 98(5), 1234-1239.

Daneshgar, P., Norouzi, P., Dousty, F., Ganjali, M.R., Moosavi-Movahedi, A.A., 2009. Dysprosium hydroxide nanowires modified electrode for determination of rifampicin drug in human urine and capsules by adsorptive square wave voltammetry. Current Pharmaceutical Analysis 5(3), 246-255.

Faria, A.F., De Souza, M.V., Bruns, R.E., De Oliveira, M.A., 2010. Simultaneous determination of first-line anti-tuberculosis drugs by capillary zone electrophoresis using direct UV detection. Talanta 82(1), 333-339.

Gan, T., Shi, Z., Wang, K., Sun, J., Lv, Z., Liu, Y., 2015. Rifampicin determination in human serum and urine based on a disposable carbon paste microelectrode modified with a hollow manganese oxide@ mesoporous silica oxide core-shell nanohybrid. Can. J. Chem. 93(10), 1061-1068.

Goutal, S., Auvity, S., Legrand, T., Hauquier, F., Cisternino, S., Chapy, H., Saba, W., Tournier, N., 2016. Validation of a simple HPLC-UV method for rifampicin determination in plasma: Application to the study of rifampicin arteriovenous concentration gradient. J. Pharm. Biomed. Anal. 123, 173-178.

Gutiérrez-Fernández, S., Blanco-López, M., Lobo-Castañón, M.J., Miranda-Ordieres, A.J., Tuñón-Blanco, P., 2004. Adsorptive Stripping Voltammetry of Rifamycins at Unmodified and Surfactant-Modified Carbon Paste Electrodes. Electroanalysis 16(20), 1660-1666.

Hammam, E., Beltagi, A., Ghoneim, M., 2004. Voltammetric assay of rifampicin and isoniazid drugs, separately and combined in bulk, pharmaceutical formulations and human serum at a carbon paste electrode. Microchem. J. 77(1), 53-62.

Kahn, M.L., Zhang, Z.J., 2001. Synthesis and magnetic properties of CoFe {sub 2} O {sub 4} spinel ferrite nanoparticles doped with lanthanide ions. ApPhL 78(23).

Kashevsky, B.E., Agabekov, V.E., Kashevsky, S.B., Kekalo, K.A., Manina, E.Y., Prokhorov, I.V., Ulashchik, V.S., 2008. Study of cobalt ferrite nanosuspensions for low-frequency ferromagnetic hyperthermia. Particuology 6(5), 322-333.

Kawde, A.-N., Temerk, Y., Farhan, N., 2014. Adsorptive Stripping Voltammetry of Antibiotics Rifamycin SV and Rifampicin at Renewable Pencil Electrodes. Acta Chim. Slov. 61, 398-405.

Kroutvar, M., Zrenner, A., Ducommun, Y., Finley, J., Abstreiter, G., 2003. Wavelength selective data storage in InGaAs–GaAs quantum dots. physica status solidi (b) 238(2), 345-348.

Leandro, K.C., Carvalho, J.M.d., Giovanelli, L.F., Moreira, J.C., 2009. Development and validation of an electroanalytical methodology for determination of isoniazid and rifampicin content in pharmaceutical formulations. Braz. J. Pharm. Sci. 45(2), 331-337.

Liu, Z., Yin, P., Gong, H., Li, P., Wang, X., He, Y., 2012. Determination of rifampicin based on fluorescence quenching of GSH capped CdTe/ZnS QDs. JLum 132(9), 2484-2488.

Lomillo, M.A., Kauffmann, J., Martinez, M.A., 2003. HRP-based biosensor for monitoring rifampicin. Biosens. Bioelectron. 18(9), 1165-1171.

Lomillo, M.A.A., Renedo, O.D., Martínez, M.J.A., 2005. Optimization of a cyclodextrin-based sensor for rifampicin monitoring. Electrochim. Acta 50(9), 1807-1811.

Mansuri, S.S., Pathak, A., Rajput, S.J., 2014. Development and validation of chemometric assisted UV Spectrophotometric and RPLC-PDA methods for the simultaneous In Vitro analysis of Isoniazid, Rifampicin and Piperine In Their Pharmaceutical Formulation. IAJPR 4(1), 540-553.

Miller, J.C., Miller, J.N., 1993. Statistics for analytical chemistry. New York: Ellis Harwood.

Misra, R.D., 2008. Quantum dots for tumor-targeted drug delivery and cell imaging.

Montemayor, S.M., García-Cerda, L., Torres-Lubián, J., 2005. Preparation and characterization of cobalt ferrite by the polymerized complex method. MatL 59(8), 1056-1060.

Prasanthi, B., Ratna, J.V., Phani, R.C., 2015. Development and validation of RP-HPLC method for simultaneous estimation of rifampicin, isoniazid and pyrazinamide in human plasma. J. Anal. Chem. 70(8), 1015-1022.

Probst, C.E., Zrazhevskiy, P., Bagalkot, V., Gao, X., 2013. Quantum dots as a platform for nanoparticle drug delivery vehicle design. Adv. Drug Del. Rev. 65(5), 703-718.

Ramaswamy, S., Musser, J.M., 1998. Molecular genetic basis of antimicrobial agent resistance inMycobacterium tuberculosis: 1998 update. Tuber. Lung Dis. 79(1), 3-29.

Rashad, M., Mohamed, R., El-Shall, H., 2008. Magnetic properties of nanocrystalline Sm-substituted CoFe2O4 synthesized by citrate precursor method. J. Mater. Process. Technol. 198(1), 139-146.

Rastgar, S., Shahrokhian, S., 2014. Nickel hydroxide nanoparticles-reduced graphene oxide nanosheets film: Layer-by-layer electrochemical preparation, characterization and rifampicin sensory application. Talanta 119, 156-163.

Ren, Y., Rivera, J.G., He, L., Kulkarni, H., Lee, D.-K., Messersmith, P.B., 2011. Facile, high efficiency immobilization of lipase enzyme on magnetic iron oxide nanoparticles via a biomimetic coating. BMC Biotechnol. 11(1), 1.

Roushani, M., Abdi, Z., 2014. Novel electrochemical sensor based on graphene quantum dots/riboflavin nanocomposite for the detection of persulfate. Sens. Actuators B Chem. 201, 503-510.

Shewiyo, D., Kaale, E., Risha, P., Dejaegher, B., Smeyers-Verbeke, J., Vander Heyden, Y., 2012. Optimization of a reversed-phase-high-performance thin-layer chromatography method

for the separation of isoniazid, ethambutol, rifampicin and pyrazinamide in fixed-dose combination antituberculosis tablets. J. Chromatogr. 1260, 232-238.

Song, J., Li, J., Li, X., Xu, L., Dong, Y., Zeng, H., 2015. Quantum Dot Light-Emitting Diodes Based on Inorganic Perovskite Cesium Lead Halides (CsPbX3). Adv. Mater. 27(44), 7162-7167.

Tang, D., Yuan, R., Chai, Y., An, H., 2007. Magnetic-Core/Porous-Shell CoFe2O4/SiO2 Composite Nanoparticles as Immobilized Affinity Supports for Clinical Immunoassays. Adv. Funct. Mater. 17(6), 976-982.

Varma, P.R., Manna, R.S., Banerjee, D., Varma, M.R., Suresh, K., Nigam, A., 2008. Magnetic properties of CoFe 2 O 4 synthesized by solid state, citrate precursor and polymerized complex methods: A comparative study. JAllC 453(1), 298-303.

Védaste, K., Egide, K., Claver, K., Kaale, E., 2014. Development and validation of high-performance thin-layer chromatographic method for the simultaneous determination of rifampicin, isoniazid, and pyrazinamide in a fixed dosage combination tablet. JPC J. Planar Chromatogr. - Mod. TLC 27(5), 392-397.

Vu, D., Koster, R., Bolhuis, M., Greijdanus, B., Altena, R., Nguyen, D., Brouwers, J., Uges, D., Alffenaar, J., 2014. Simultaneous determination of rifampicin, clarithromycin and their metabolites in dried blood spots using LC–MS/MS. Talanta 121, 9-17.

Wu, H., Liu, G., Wang, X., Zhang, J., Chen, Y., Shi, J., Yang, H., Hu, H., Yang, S., 2011. Solvothermal synthesis of cobalt ferrite nanoparticles loaded on multiwalled carbon nanotubes for magnetic resonance imaging and drug delivery. Acta Biomater. 7(9), 3496-3504.

Xu, H., Aguilar, Z.P., Yang, L., Kuang, M., Duan, H., Xiong, Y., Wei, H., Wang, A., 2011. Antibody conjugated magnetic iron oxide nanoparticles for cancer cell separation in fresh whole blood. Biomaterials 32(36), 9758-9765.

Xu, Y., Wei, J., Yao, J., Fu, J., Xue, D., 2008. Synthesis of CoFe2O4 nanotube arrays through an improved sol–gel template approach. MatL 62(8), 1403-1405.

Zhang, Y., Liu, Y., Yang, Z., Xiong, R., Shi, J., 2011. Synthesis of CoFe2O4 nanoparticles with tunable magnetism by the modified hydrothermal method. JNR 13(10), 4557-4563.

Figure Captions:

Fig. 1. Characterization of $CoFe_2O_4$ by FESEM with different magnification (from A to D), PVP-capped CdSe by FESEM (E and F), and PVP-capped $CoFe_2O_4$@CdSe core-shell nanoparticles by FESEM (G), TEM (from H to J) and EDX (K).

Fig. 2. Cyclic voltammograms of: (A) 10×10^{-6} molL^{-1} of RIF solution in 0.1molL^{-1} PBS (pH=2), and (B) square-wave voltammograms of 1.0×10^{-12} mol L^{-1} RIF in 0.1 mol L^{-1} PBS (pH=2) on the surface of various electrodes. Curves (a) bare GCE (b) $CoFe_2O_4$/GCE (c) PVP-capped $CoFe_2O_4$@CdSe/GCE and (d) PVP-capped $CoFe_2O_4$@CdSe/GCE in absence of analyte. Accumulation potential: −0.7 V; accumulation time: 600 s; SW frequency 25 Hz; pulse amplitude: 50 mV; step potential: 5 mV and scan rate: 50 mV s^{-1}.

Fig. 3. Cyclic voltammetric response of PVP-capped $CoFe_2O_4$@CdSe/GCE at different pH of Britton-Robinson buffer (from right to left), 1, 2, 3, 4, 5, 6 and 7; scan rate 50mVs^{-1}. Inset: (A) and (B) are the variation of the anodic peak current and formal potentials versus pH values, respectively.

Fig. 4. Effect of the accumulation pH (A), accumulation potential (B) and accumulation time (C) on the peak currents in 0.1 mol L^{-1} PBS (pH=2) containing 1.0×10^{-8} mol L^{-1} RIF; SW frequency 25 Hz, pulse amplitude: 50 mV and step potential: 5 mV.

Fig. 5. SW voltammograms of RIF at different concentrations (from inner to outer): 1.0×10^{-16}, 1.0×10^{-14}, 1.0×10^{-13}, 1.0×10^{-12}, 1.0×10^{-11}, 5.0×10^{-11}, 1.0×10^{-10}, 1.0×10^{-9}, 1.0×10^{-8} and 1.0×10^{-7} molL^{-1} under the optimum conditions at the surface of PVP-capped $CoFe_2O_4$@CdSe/GCE. Inset (A) log peak currents vs. log RIF concentrations and (B) part of enlarged view of the SW plot from concentration 1.0×10^{-16} to 1.0×10^{-11} molL^{-1}.

Table 1 Determination of RIF in drug and serum samples (n=3)

Sample	Added (nmolL^{-1})	Expected (nmolL^{-1})	Founded (nmolL^{-1})	t_{exp}	t_{tab} (95%)	Recovery%	RSD%
Tablet[a]	-	10.0	9.71±0.19	-	4.3	-	1.94
	5.0	15.0	14.96±0.16	0.34	4.3	99.73	1.09

	5.0	20.0	19.73±0.10	3.62	4.3	98.68	0.52
Serum1	5.0	5.0	4.89±0.16	-	4.3	-	3.32
	1.0	6.0	5.84±0.16	1.34	4.3	97.36	2.84
	1.0	7.0	7.10±0.18	0.77	4.3	101.45	2.62
Serum2	10.0	10.0	10.08±0.17	-	4.3	-	1.71
	1.0	11.0	10.94±0.20	0.35	4.3	99.53	1.86
	1.0	12.0	12.11±0.32	0.49	4.3	100.94	2.70

±Shows the standard deviation

t_{exp}: calculated value of Student t test, t_{tab}: t value obtained from the table of Student t test.

[a] 300 mg capsule produced by Hakim Drug Company

Highlights

- A novel electrochemical biosensor (PVP capped $CoFe_2O_4$@CdSe/GCE) was prepared by a novel synthesis method using $CoFe_2O_4$ magnetic nanoparticles (MNPs) as a core and CdSe quantum dots (QDs) as a shell.
- The fabricated biosensor can significantly enhance electrocatalytic activity towards the oxidation of rifampicin.
- The main advantage of this sensor is a wide range from 1.0×10^{-16} to 1.0×10^{-7}M and very low detection limit 4.5×10^{-17}M compared with previously reported voltammetric methods.
- The wide linear range, biocompatibility, very low detection limit, good selectivity, and high electrochemical performance of the PVP-capped $CoFe_2O_4$@CdSe make it a promising candidate as a novel platform for fabrication of electrochemical biosensors and further sensor applications.

Fig. 1

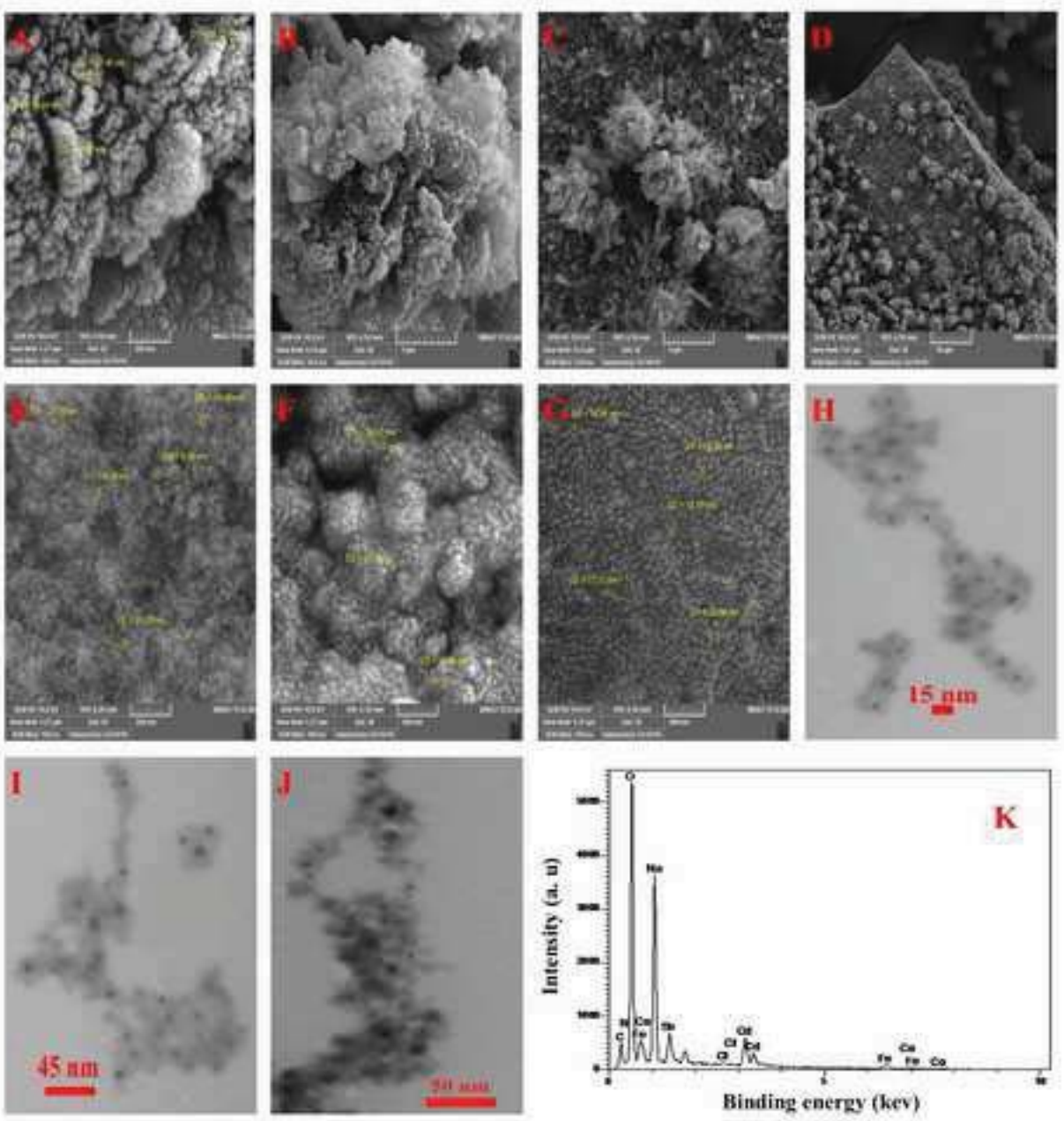

Fig. 2

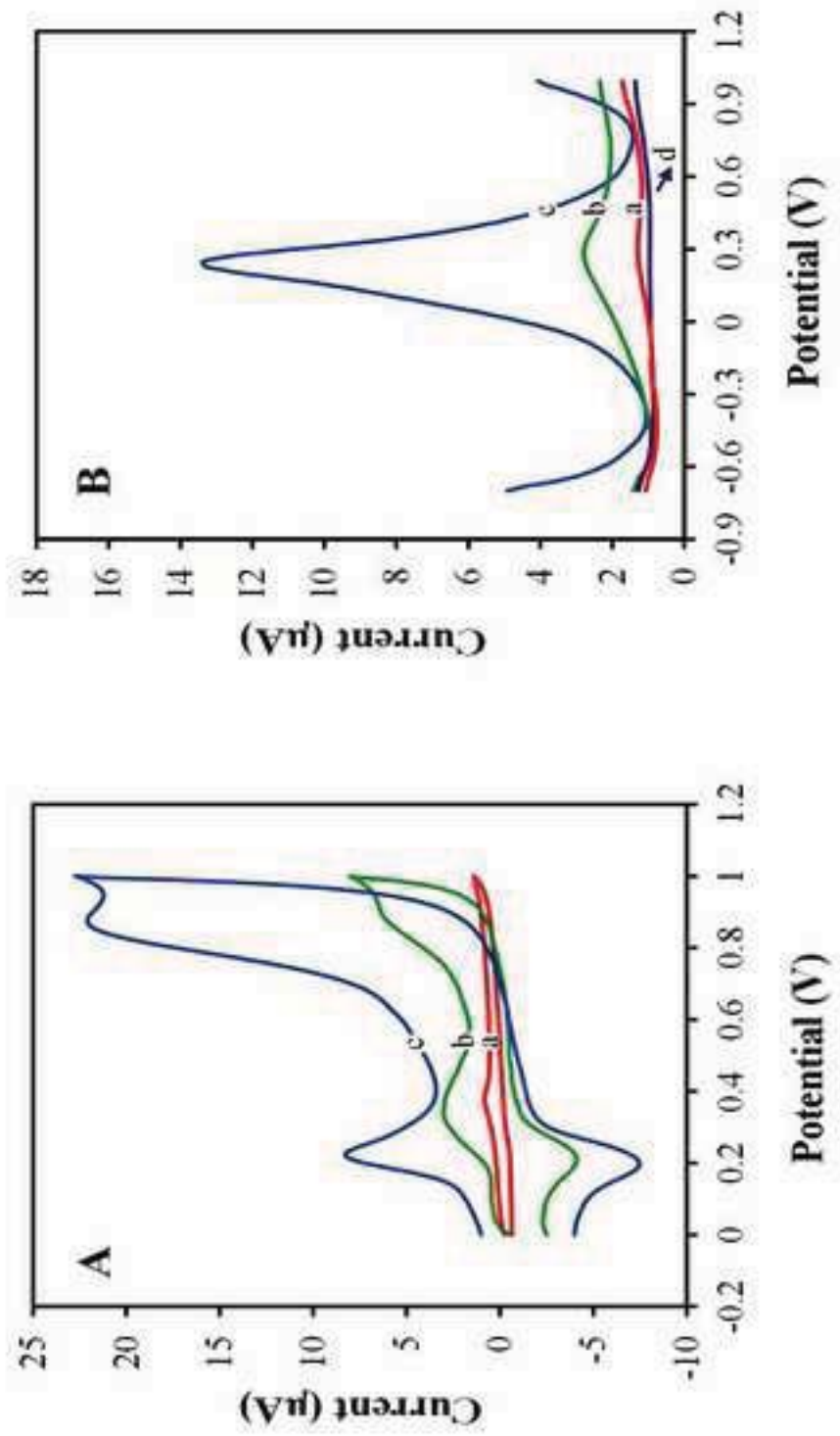

Figure 2

Fig. 3

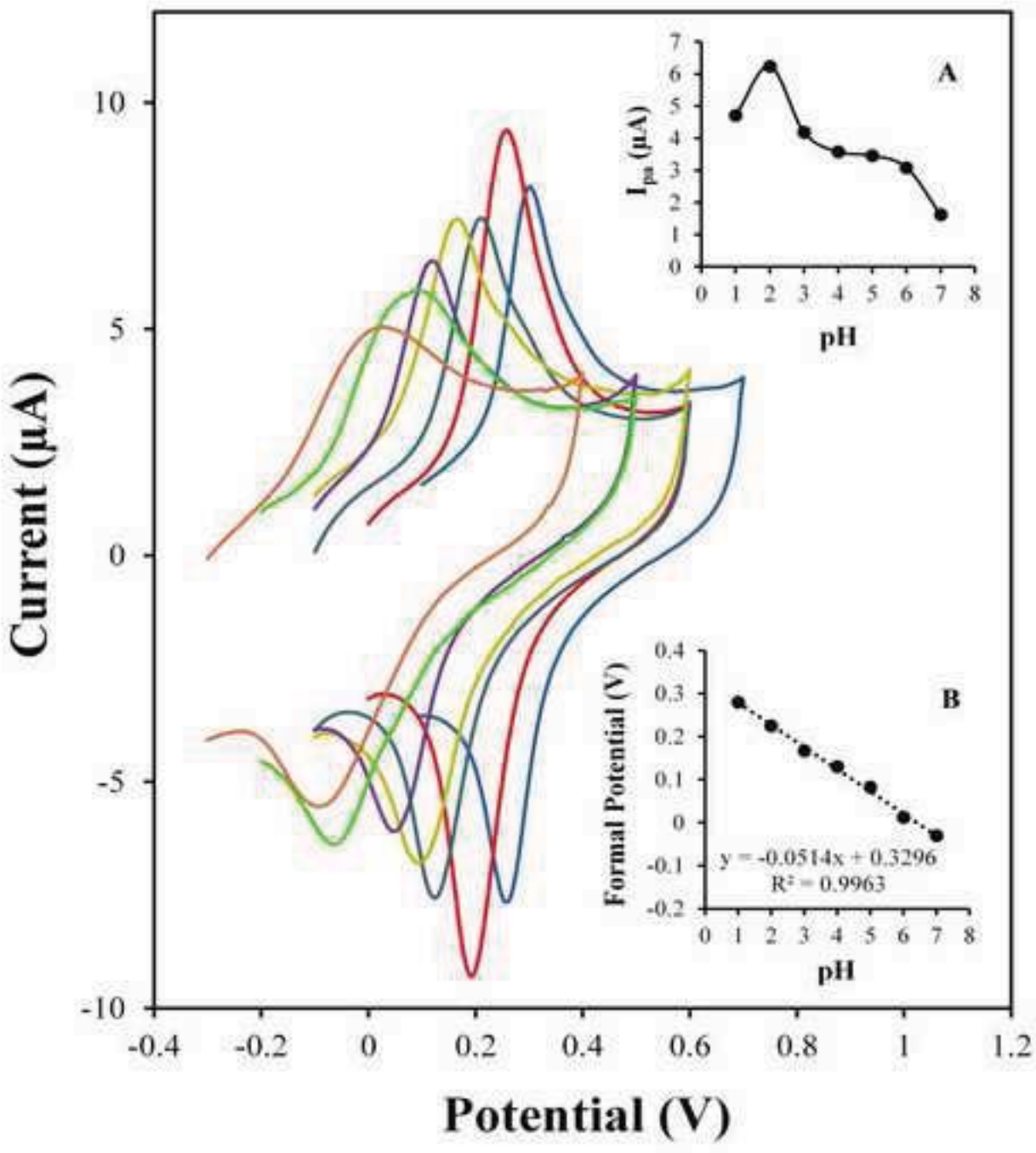

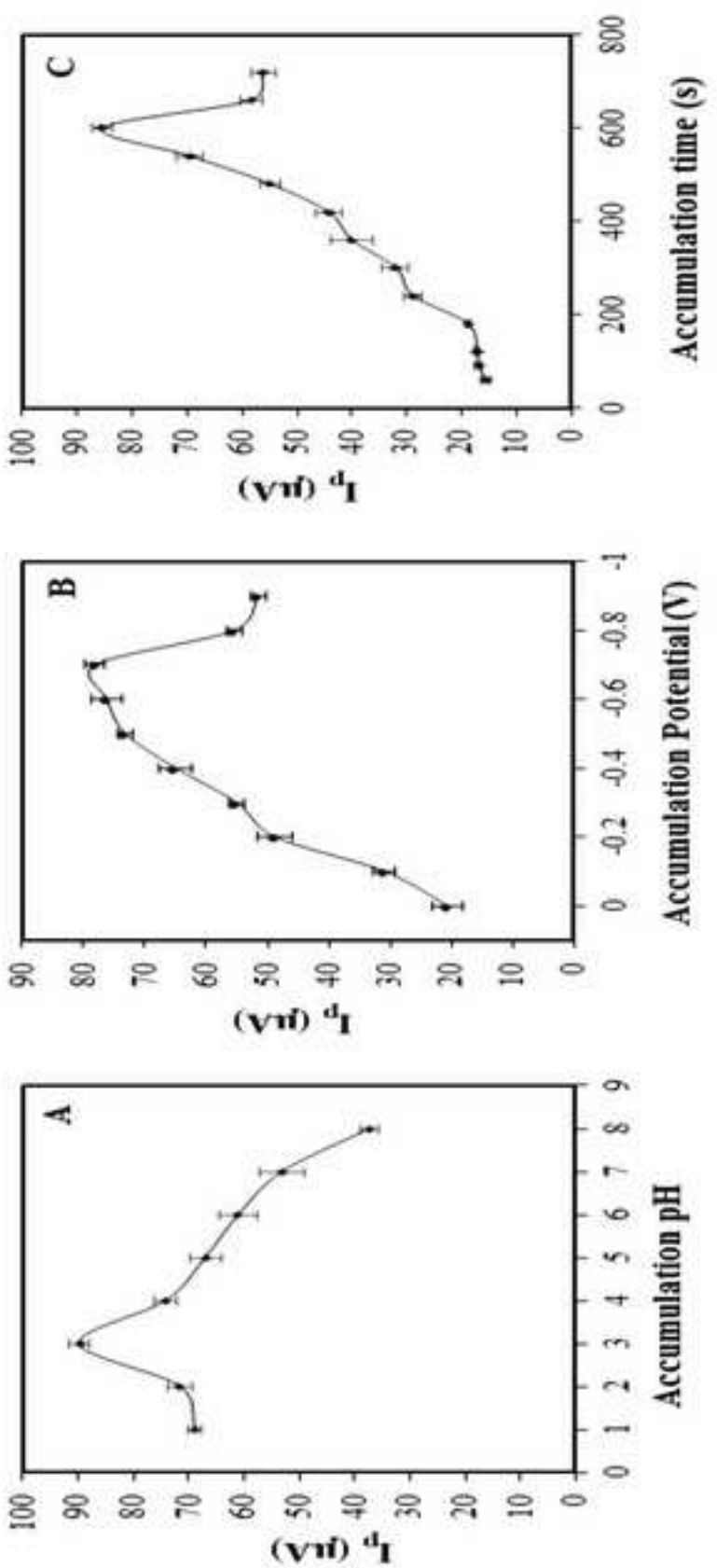

Fig. 4

Figure 4

Fig. 5